Supporting information:

Table S1. ADME characteristics of compounds **3a-3c**.

Entry	Compounds		
	3a	**3b**	**3c**
Physicochemical Properties / Lipophilicity / Druglikeness			
Molecular weight (g/mol)	435.31	500.98	543.02
Num. heavy atoms	30	37	40
Num. arom. Heavy atoms	23	31	34
Fraction Csp3	0.0	0.0	0.0
Num. rotatable bonds	6	6	8
Num. H-bond acceptor	3	3	4
Num. H-bond donors	1	1	1
Molar Refractivity	120.19	150.19	157.74
TPSA ($Å^2$)	59.28	59.28	77.10
Consensus Log $P_{o/w}$	5.07	6.26	5.83
Lipinski's Rule	Yes	No	No
Bioavailability Score	0.55	0.17	0.17
Veber	Yes	Yes	Yes
PAINS filters	0	0	0
Pharmacokinetics			
GI absorption	High	Low	Low
BBB permeant	No	No	No
P-gp substrate	No	No	No
CYP1A2 inhibitor	No	No	No
CYP2C19 inhibitor	Yes	No	No
CYP2C9 inhibitor	Yes	No	No
CYP2D6 inhibitor	No	No	No
CYP3A4 inhibitor	No	No	No
Log K_p (cm/s)	-4.66	-3.92	-4.60

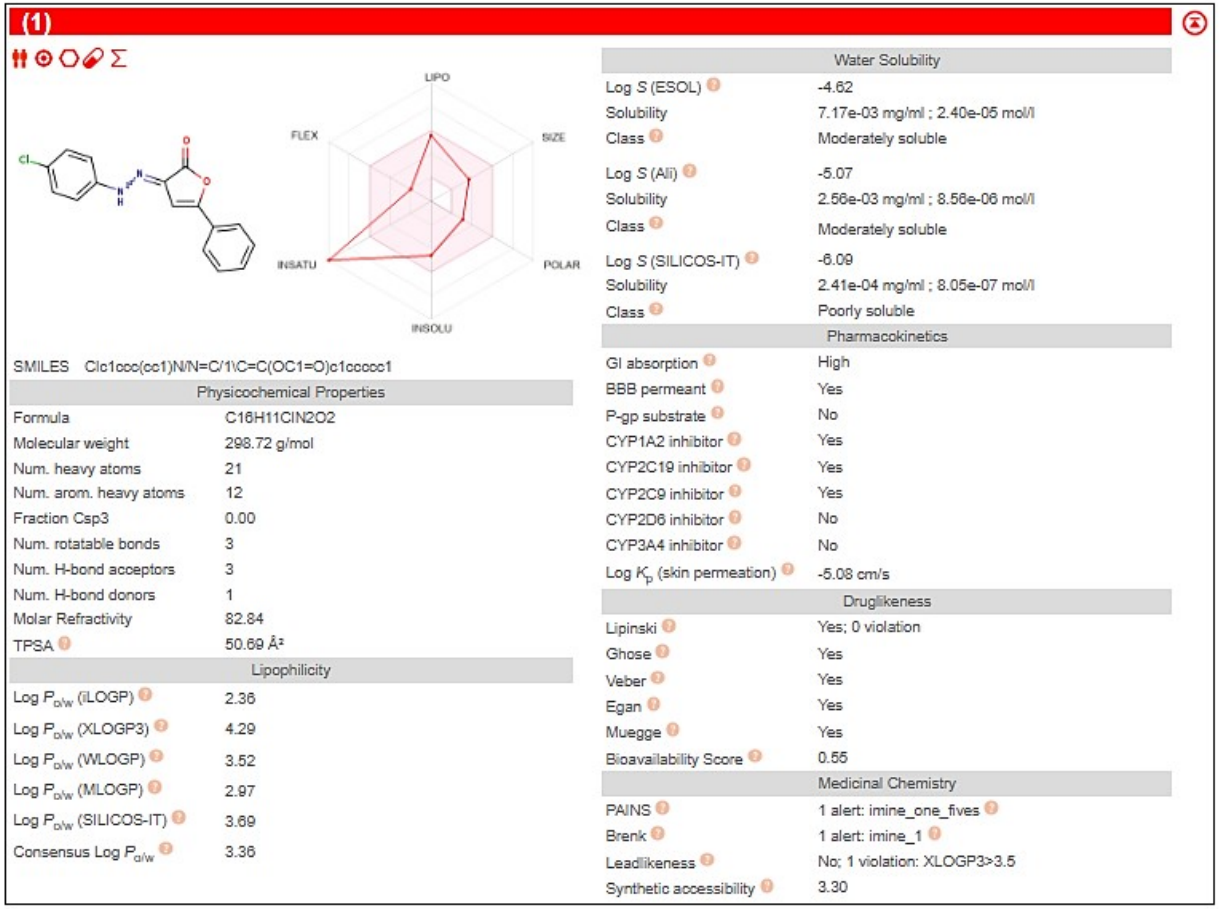

Fig. S1. ADME profile of compound **1**.

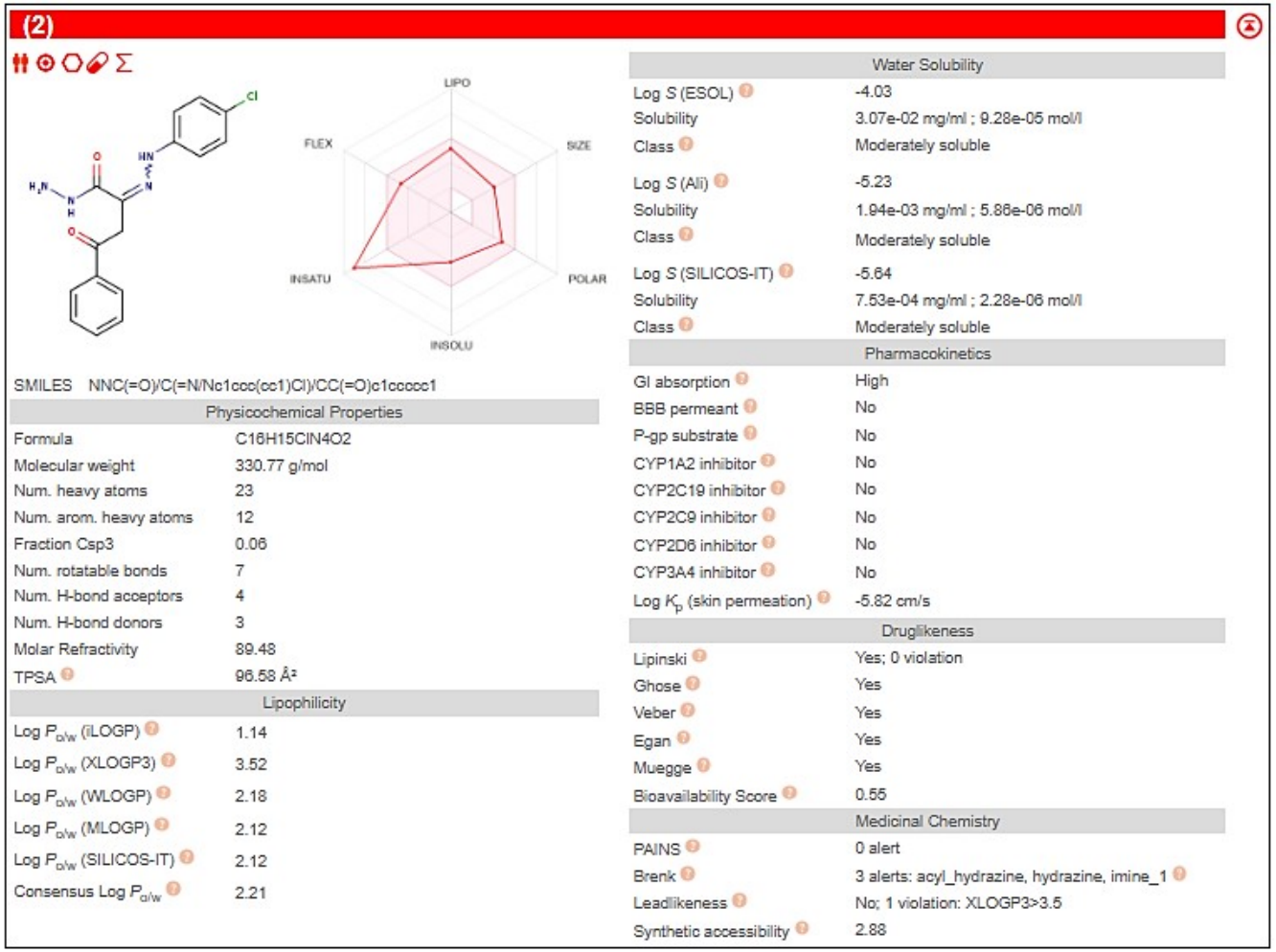

Fig. S2. ADME profile of compound **2**.

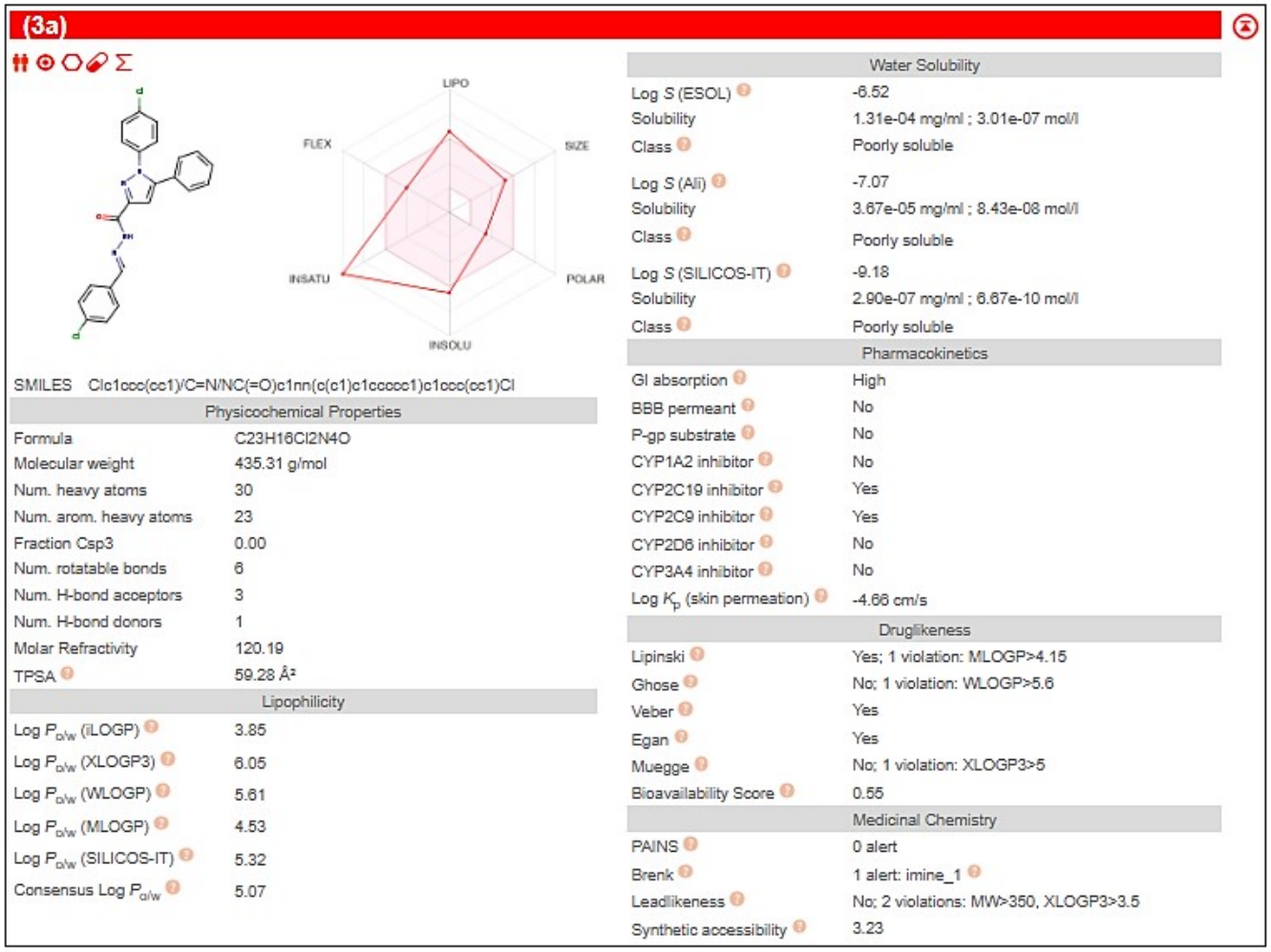

Fig. S3. ADME profile of compound **3a**.

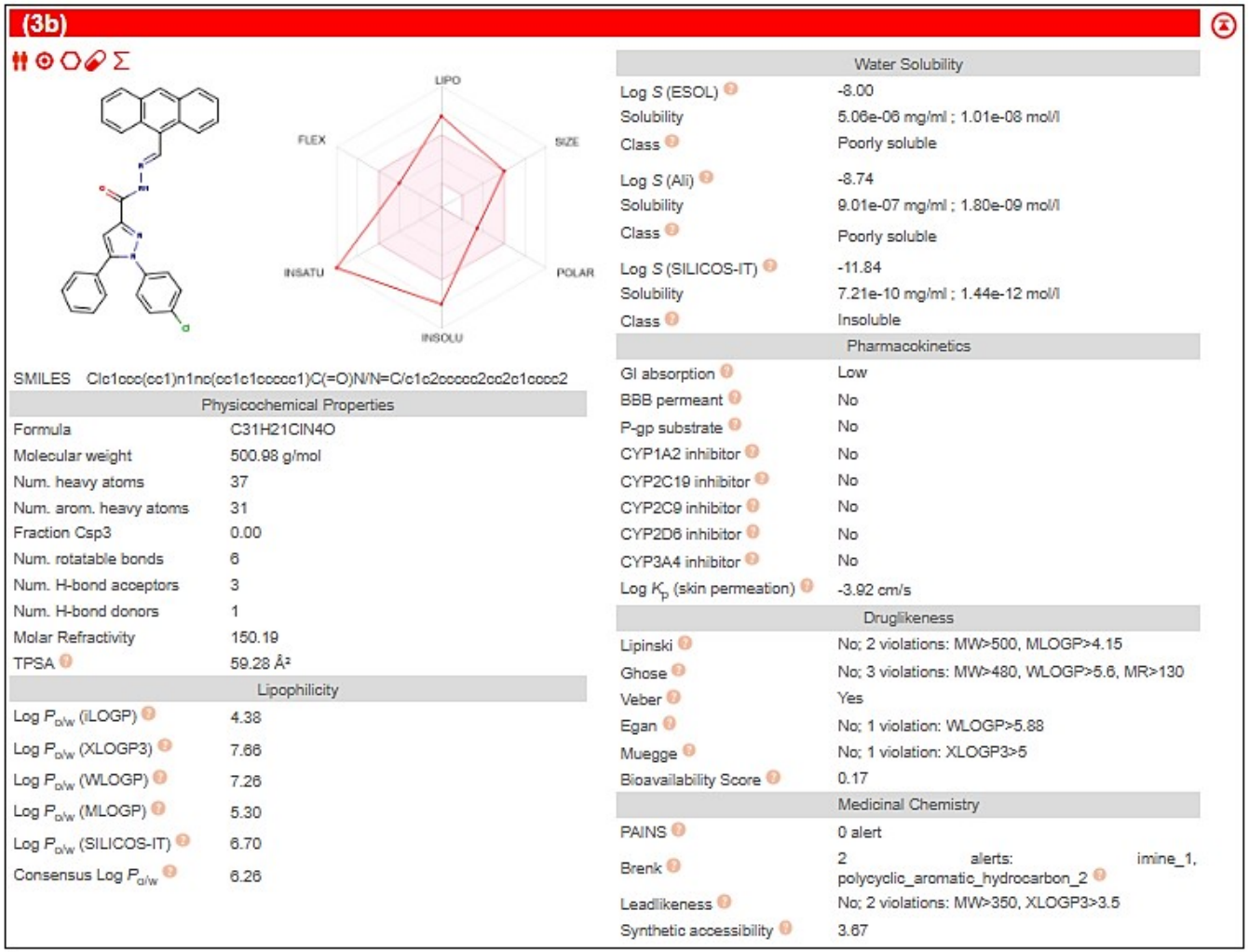

Fig. S4. ADME profile of compound **3b**.

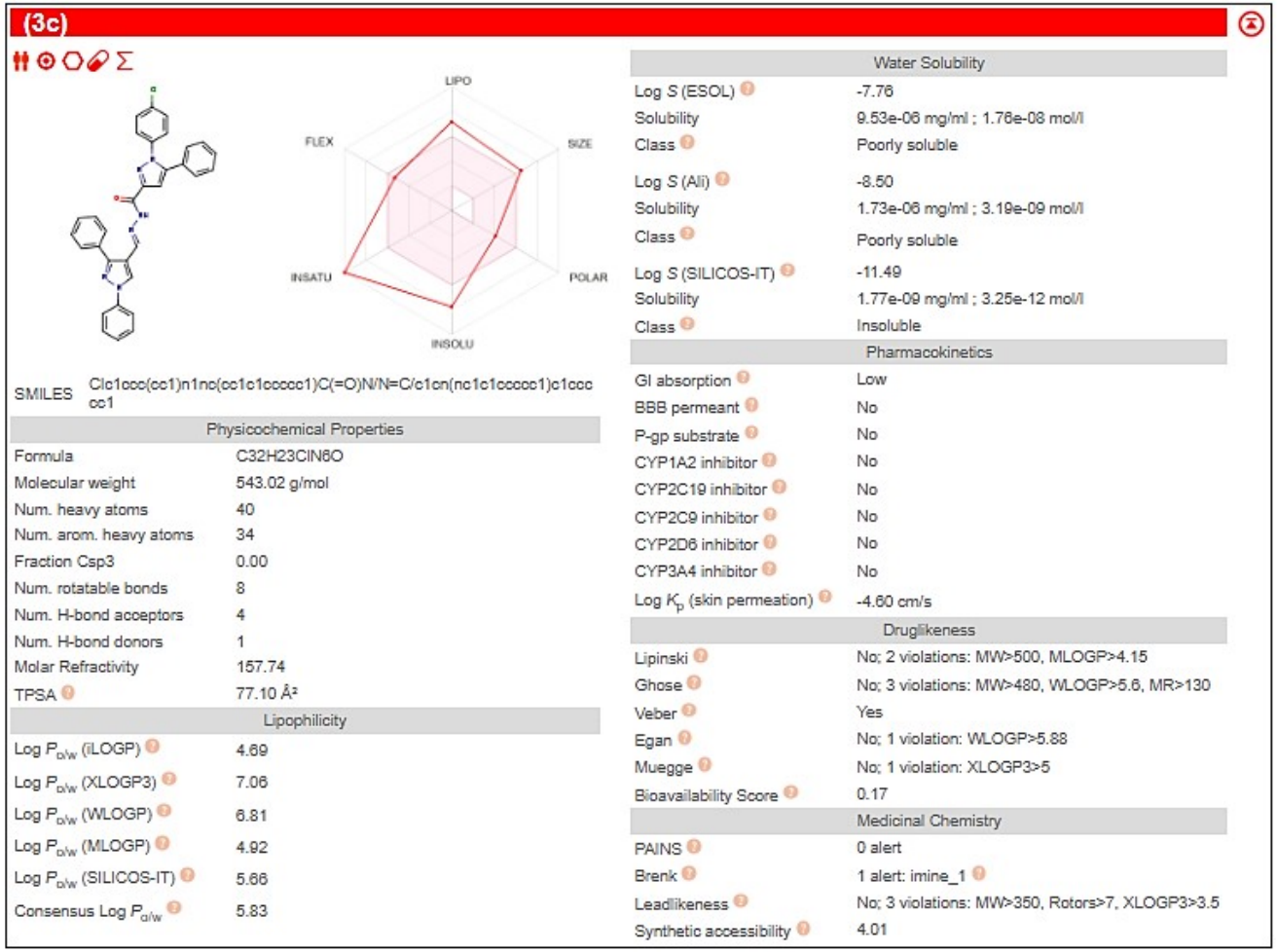

Fig. S5. ADME profile of compound **3c**.

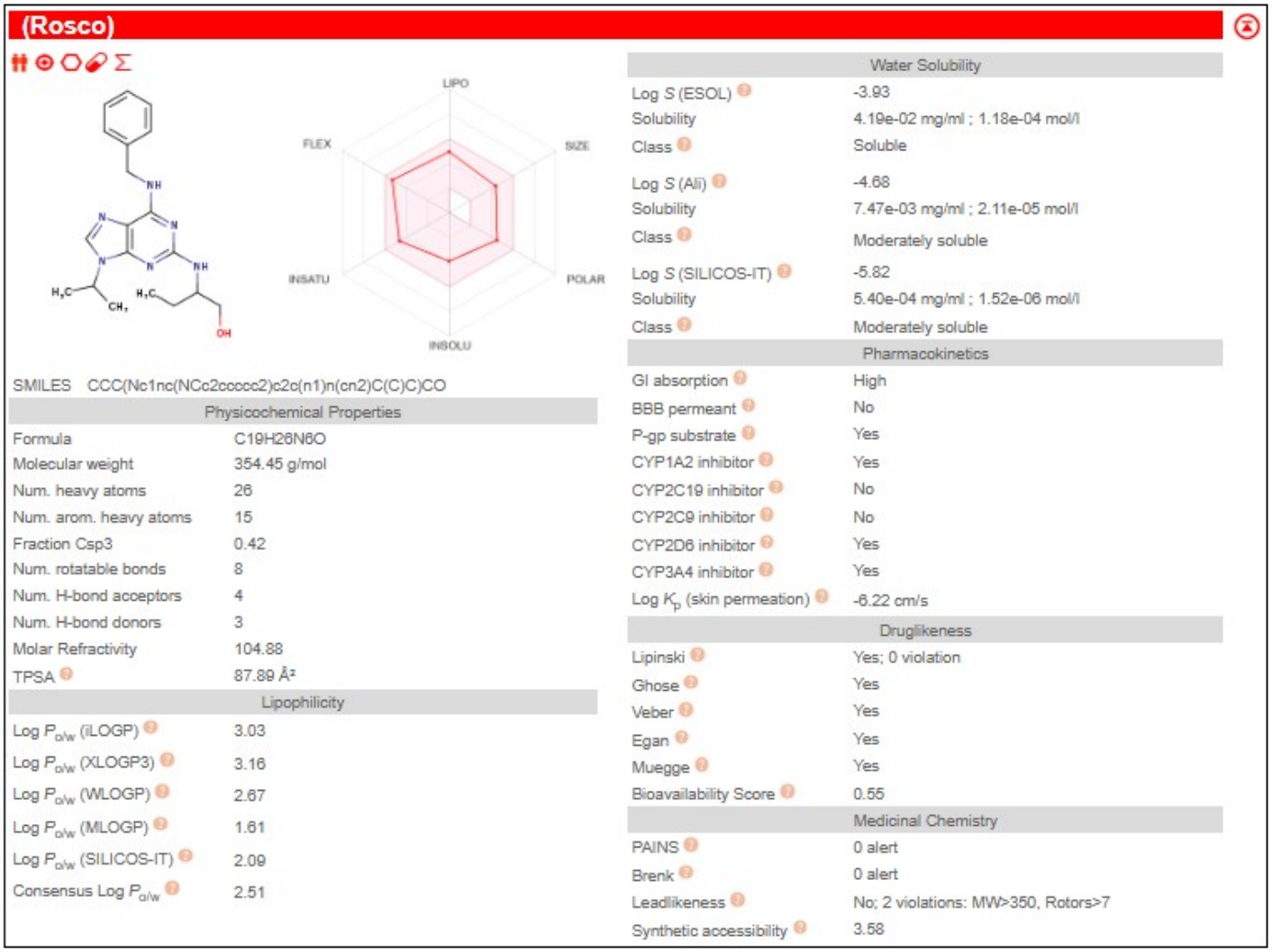

Fig. S6. ADME profile of Roscovitine.

Materials and methods

Melting points (°C) were determined using a MEL-TEMP II digital melting point apparatus. Infrared (IR) spectra were obtained from KBr pellets employing a Thermo Electron Nicolet 7600 FT-IR spectrometer (USA) at Faculty of Science, Ain Shams University. Proton and carbon nuclear magnetic resonance (^{1}H and ^{13}C NMR) spectra were recorded at 400 and 100 *MHz* on a BRUKER NMR spectrometer, using tetramethyl silane (TMS) as an internal reference and deuterated dimethyl sulfoxide (DMSO-d_6) as the solvent, at the Faculty of Pharmacy, Ain Shams University. Electron impact mass spectra (EI-MS) were obtained at an ionization energy of 70 eV using a direct probe inlet coupled to a single-quadrupole mass spectrometer (Thermo Scientific GC–MS, ISQ LT model) operated with Thermo X-CALIBUR software at the Regional Center for Mycology and Biotechnology (RCMB), Al-Azhar University, Cairo, Egypt. Elemental (CHN) analyses were carried out at the Faculty of Science, Ain Shams University, employing a Perkin-Elmer 2400 elemental analyzer. The progress of reactions and purity of newly synthesized compounds were assessed by thin-layer chromatography (TLC) using silica gel $60F_{254}$ precoated aluminum sheets (Merck), with visualization of spots under ultraviolet (UV) light using diethyl ether as mobile phase.

We monitored the impurity profile of the reactions throughout the synthetic sequence to ensure the reliability and reproducibility of the reported methodology. In the hydrazinolysis step, the primary impurity observed was trace amounts of unreacted starting materials, which were readily removed by recrystallization from the proper solvent. No significant side products associated with over reaction or hydrazine mediated ring opening were detected under the optimized conditions. Overall, the reactions demonstrated a clean impurity profile, and the purification protocols described (TLC, filtration, and recrystallization as needed) consistently afforded analytically pure materials. Characterization by elemental and spectral analysis confirmed the absence of persistent or structurally ambiguous impurities across the synthesized series.

The synthetic transformations described in our work were carried out on a laboratory scale, typically using reaction batches in the range of 2.0 mmol of the hydrazide and substituted aldehydes. Within this scale, all steps, including hydrazinolysis and subsequent condensation with the selected aromatic aldehydes, proceeded cleanly and reproducibly without requiring specialized reaction conditions. Although we did not perform a formal scale up study, the synthetic operations involved rely on straightforward, well established organic reactions (hydrazinolysis followed by

Schiff base formation). These reactions use readily available reagents, mild temperatures, and simple workup procedures, suggesting that the methodology should be amenable to larger scale preparation. Additionally, we observed consistent yields and product purity across repeated experiments, indicating good robustness of the designed sequence under standard laboratory conditions.

Reaction of hydrazide 2 with aldehydes

A solution of acid hydrazide **2** [30] (2 mmol) and aromatic aldehydes namely, 4-chlorobenzaldehyde, anthracene-9-carbaldehyde, and 1,3-diphenylpyrazole-4-carbaldehyde (2 mmol) in an absolute ethyl alcohol (20 mL) was refluxed for 3-4 h (TLC: Et_2O/AcOEt, 2:1). The solid precipitated was collected and recrystallized by 1,4-dioxane to get pyrazole derivatives **3a-3c**, respectively.

N'-(4-Chlorobenzylidene)-1-(4-chlorophenyl)-5-phenyl-1H-pyrazole-3-carbohydrazide (3a)

Yellow crystals, mp. 178-180 ^oC, yield 79%. FT-IR, KBr (ν, cm^{-1}): 3215 (NH), 1651 (C=O). ^1H NMR, 400 *MHz* (DMSO-d_6, δ, ppm): 7.16-8.27 (m, 13H, phenyl-H), 8.76 (s, 1H, C4-H pyrazole), 9.02 (s, 1H, CH=N), 11.61 (*br*.s, 1H, NH). ^{13}C NMR, 100 *MHz* (DMSO-d_6, δ, ppm): 107.3, 107.4, 110.1, 110.2, 116.7, 121.2 (2), 121.8 (2), 128.6 (2), 128.7 (2), 133.2 (2), 133.3 (2), 134.9, 135.0, 143.5, 156.7, 156.8, 166.9. EI-MS, 70 eV (*m/z*, %): 434.50 ($M^{+\cdot}$, 17), 373.93 (7), 351.67 (8), 314.36 (15), 271.31 (26), 194.26 (8), 101.64 (11), 76.96 (100). Anal. Calcd. for $C_{23}H_{16}Cl_2N_4O$ (435.31): C, 63.46; H, 3.70; N, 12.87%; Found: C, 63.31; H, 3.61; N, 12.89%.

N'-(Anthracen-9-ylmethylene)-1-(4-chlorophenyl)-5-phenyl-1H-pyrazole-3-carbohydrazide (3b)

Yellow crystals, mp. 248-250 ^oC, yield 74%. FT-IR, KBr (ν, cm^{-1}): 3228 (NH), 1660 (C=O). ^1H NMR, 400 *MHz* (DMSO-d_6, δ, ppm): 7.29-8.23 (m, 17H, Ar-H), 8.58 (s, 1H, C4-H pyrazole), 8.98 (s, 1H, C10-H anthracene), 9.28 (s, 1H, CH=N), 11.75 (*br*.s, 1H, NH). ^{13}C NMR, 100 *MHz* (DMSO-d_6, δ, ppm): 115.0, 115.1, 121.2, 123.7 (2), 125.4 (2), 125.5, 125.6 (2), 127.6 (2), 129.3 (2), 129.7 (2), 129.8, 130.0 (2), 130.1 (2), 131.3,

133.5, 134.6, 137.7, 137.8, 141.0, 141.1, 149.9, 155.3, 168.6. EI-MS, 70 eV (*m/z*, %): 500.92 ($M^{+\cdot}$, 16), 419.14 (95), 351.03 (78), 289.08 (42), 211.16 (100), 121.13 (88), 84.58 (65). Anal. Calcd. for $C_{31}H_{21}ClN_4O$ (500.99): C, 74.32; H, 4.23; N, 11.18%; Found: C, 74.23; H, 4.18; N, 11.16%.

1-(4-Chlorophenyl)-N'-((1,3-diphenyl-1H-pyrazol-4-yl)methylene)-5-phenyl-1H-pyrazole-3-carbohydrazide (3c)

Yellow crystals, mp. 224-226 ^oC, yield 71%. FT-IR, KBr (ν, cm^{-1}): 3211 (NH), 1661 (C=O). ^1H NMR, 400 *MHz* (DMSO-d_6, δ, ppm): 7.06-8.05 (m, 19H, Ar-H), 8.81 (s, 1H, C4-H pyrazole), 8.97 (s, 1H, C5-H pyrazole), 9.16 (s, 1H, CH=N), 11.21 (*br*.s, 1H, NH). ^{13}C NMR, 100 *MHz* (DMSO-d_6, δ, ppm): 117.2, 119.2, 119.3 (2), 126.2, 126.5, 127.3, 127.5 (2), 127.6 (2), 128.2, 128.4 (2), 128.8, 129.1, 129.2 (2), 130.1, 130.2 (2), 132.4, 132.5 (2), 134.2, 139.4, 139.5 (2), 152.0, 152.1, 174.3. EI-MS, 70 eV (*m/z*, %): 543.01 ($M^{+\cdot}$, 47), 390.28 (42), 301.60 (35), 256.34 (100), 200.55 (41), 134.22 (56), 129.70 (71), 102.63 (23). Anal. Calcd. for $C_{32}H_{23}ClN_6O$ (543.03): C, 70.78; H, 4.27; N, 15.48%; Found: C, 70.68; H, 4.21; N, 15.50%.

MTT assay

The mentioned cell lines were used to explore the inhibitory effects of substances on cell growth using the MTT assay. This colorimetric assay was based on the conversion of the yellow tetrazolium bromide (MTT) to a purple formazan derivative by mitochondrial succinate dehydrogenase in viable cells. The stock samples of the substances were diluted with RPMI-1640 medium to desired concentrations ranging from 1.56 to 100 µM. The final concentration of DMSO in each sample did not exceed 1% (v/v). Doxorubicin was used as positive control and DMSO was employed as a negative control. Cell lines were cultured in RPMI-1640 medium with 10% fetal bovine serum. Antibiotics added were 100 units/mL penicillin and 100 µM streptomycin at 37^oC in a 5% CO_2 incubator. The cell lines were seeded on a 96-well plastic plate at a density of 1.0 x 10^4 cells / well at 37^oC for 48 h under 5% CO_2. After incubation, the cells were treated with different concentrations of substances and incubated for 48 h. After that, 20 µL of MTT solution at 5 mg/mL was added and incubated for 4 h. DMSO in volume of 100 µL was added into each well to dissolve the purple formazan formed. The colorimetric assay was measured and recorded at absorbance of 570 nm using a plate reader (EXL 800, USA). The

relative cell viability in percentage was calculated as (A_{570} of treated samples / A_{570} of untreated sample) x 100. The IC_{50} values were determined according to the equation of Boltzmann sigmoidal concentration-response curves utilizing the non-linear regression fitting model.

In Silico Target Prediction

The plausible molecular targets of substrates were predictable applying SwissTargetPrediction (http://www.swisstargetprediction.ch). The SMILES account of the substrates was stored into the tool, and predictions were made based on both 2D and 3D matched to recognized ligands. Just targets with a high prospect score were judged for further validation.

Molecular docking

Molecular docking is a powerful computational approach for elucidating the interactions between synthesized compounds and key amino acid residues within the active site of a target receptor using Autodock Vina. In this study, the binding tendencies of the prepared ligands toward CDK2 were assessed by comparing their calculated docking scores. The potent derivatives **3a–3c** were constructed using ChemBio3D Ultra 14.0, followed by partial charge assignment and energy minimization according to established protocols. The crystal structure of target protein was retrieved from protein data bank (PDB ID: 2A4L), then prepared by correction, hydrogen addition, and energy minimization. Subsequently, docking simulations were performed to predict the binding modes and affinities of the candidate compounds within the CDK2 active site. The co-crystallized ligand (RRC) was employed as a reference standard, and all docking parameters were set in accordance with previously described conditions.

Molecular Dynamics Simulation

Molecular dynamics simulations were operated to complement the docking study and to examine the time-dependent stability of ligand-protein complexes. The docked poses of the selected compounds were simulated together with doxorubicin as a reference drug and the co-crystallized ligand (RRC) over a 100 ns time scale using the Desmond program. System preparation included protein optimization, solvation in an explicit TIP3P water environment, and charge neutralization by the addition of counterions. The complexes were placed in an orthorhombic simulation

box under periodic boundary conditions and described using the OPLS force field. Following energy minimization and equilibration, production runs were carried out under NPT conditions at 300 K and 1 atm. The resulting trajectories were analyzed in terms of RMSD, RMSF, and protein-ligand interaction patterns.

ADME Profiling

The ADME properties of all substrates were explored by the SwissADME free web tool (http://www.swissadme.ch/index.php).

Statistical analysis

The bioassay was repeated in triplicate. The data obtained were presented as means ± standard error of the means (SEM) (n = 3) using SPSS 13.0 program (SPSS Inc., Chicago, IL). Differences between groups were considered statistically significant at p values < 0.05.

Spectral data

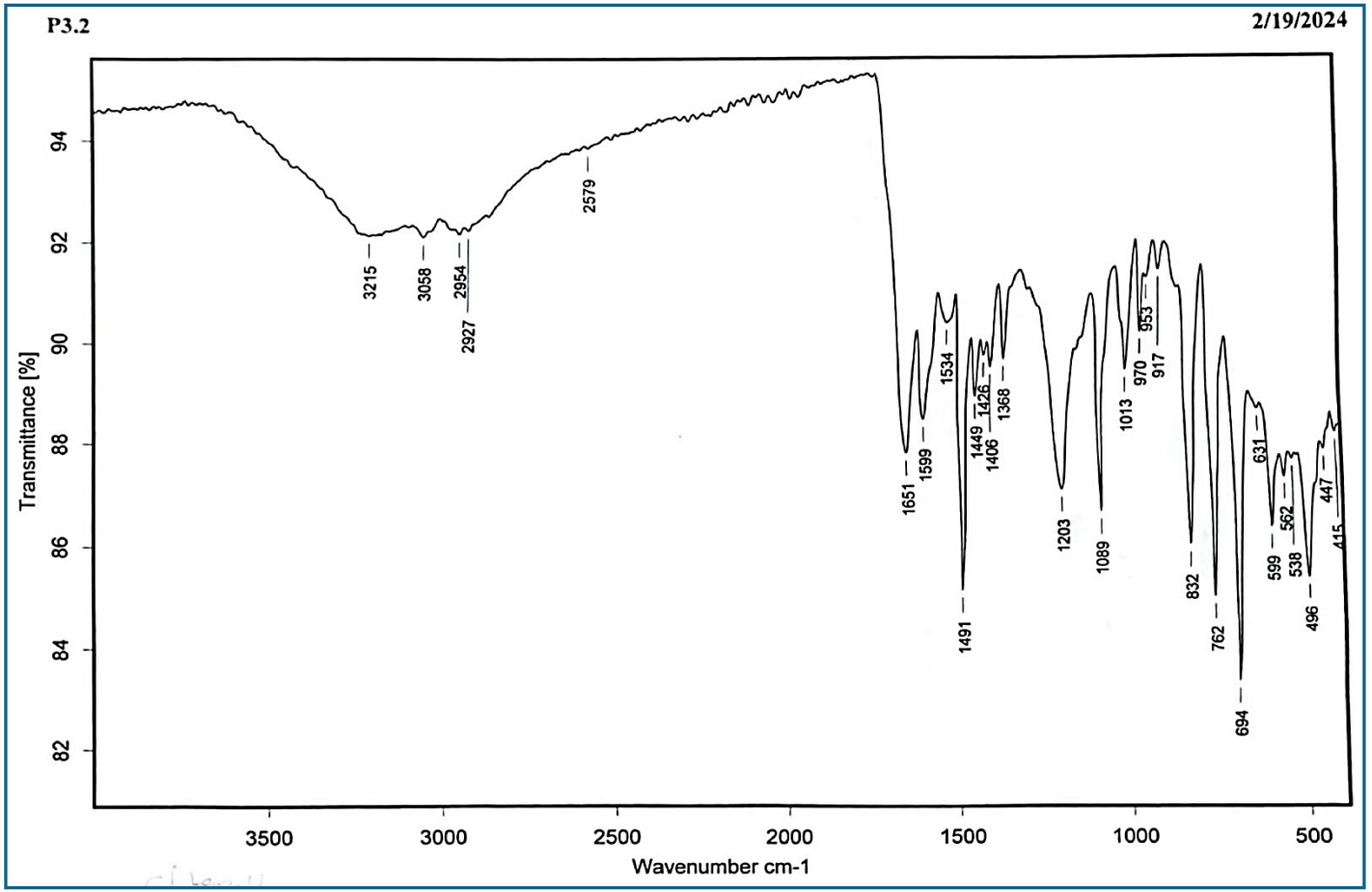

FTIR spectrum of compound **3a**

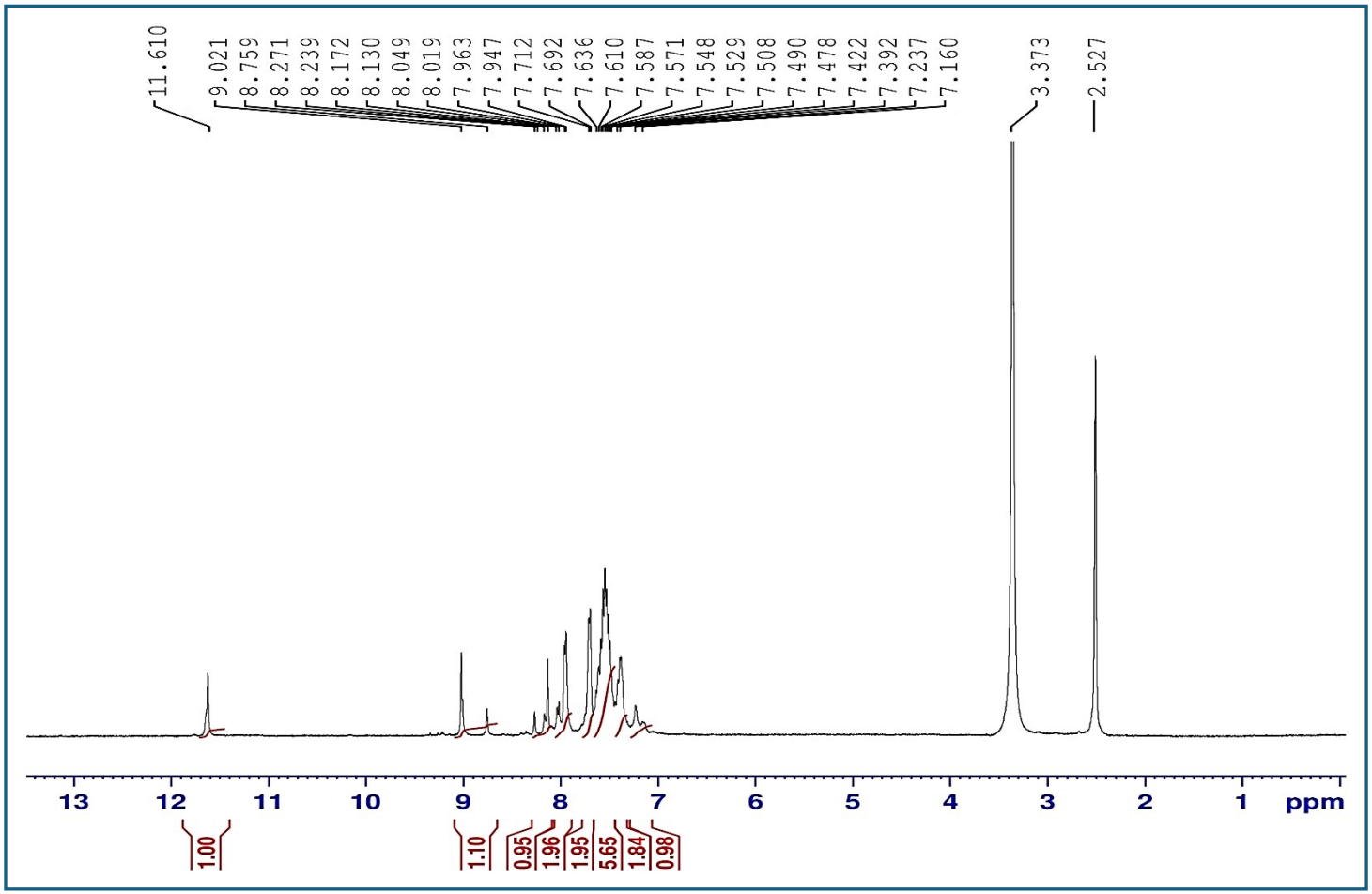

^{1}H NMR spectrum (DMSO-d_6) of compound **3a**

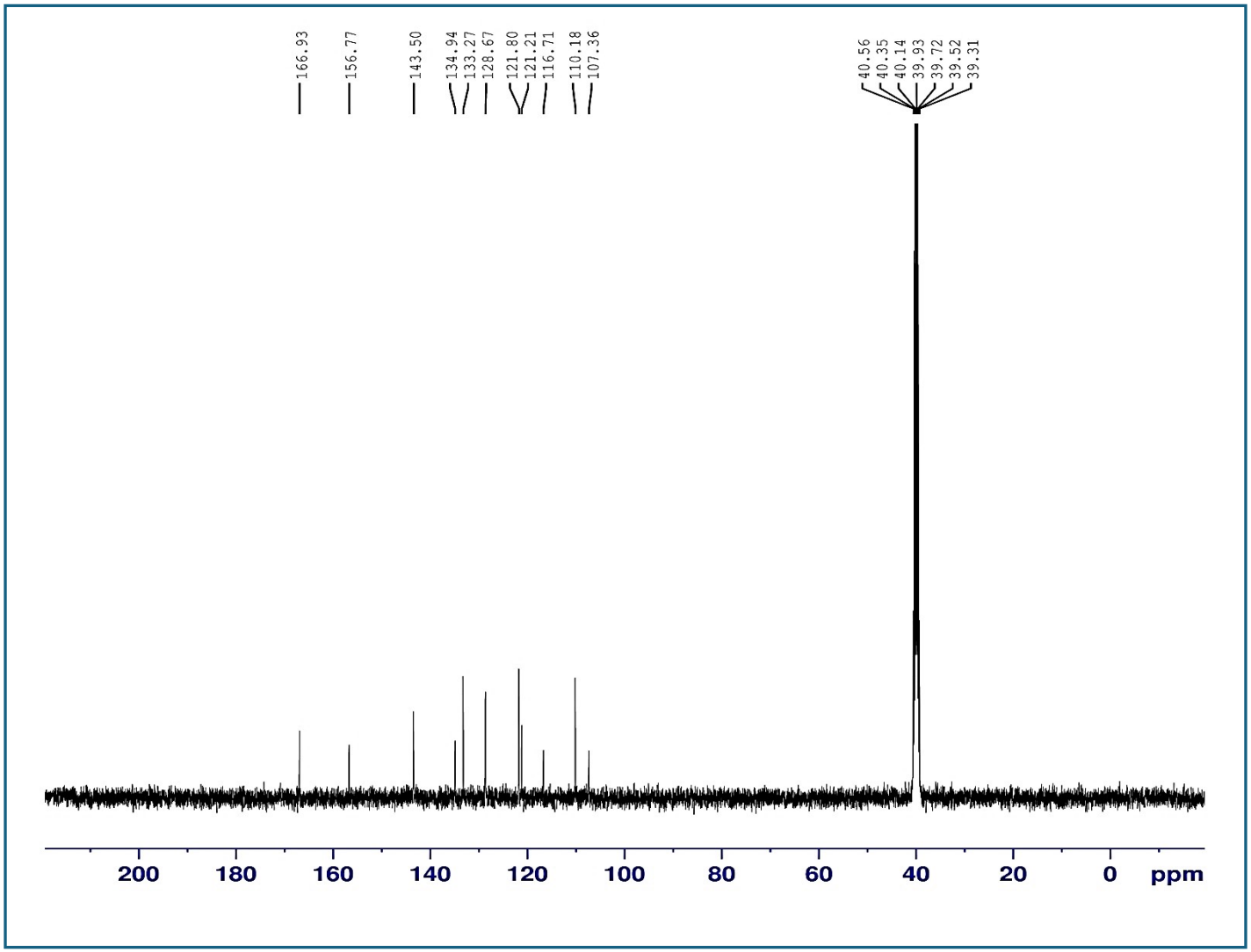

^{13}C NMR spectrum (DMSO-d_6) of compound **3a**

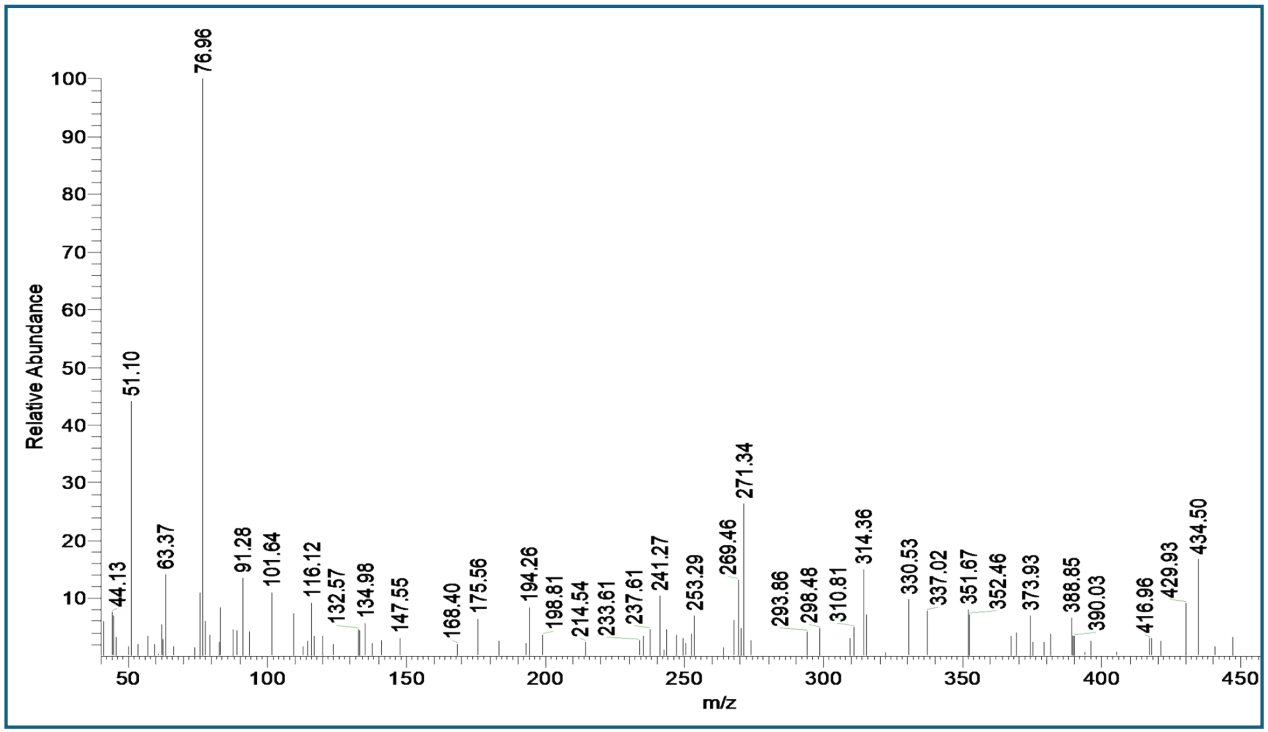

GCMS of compound **3a**

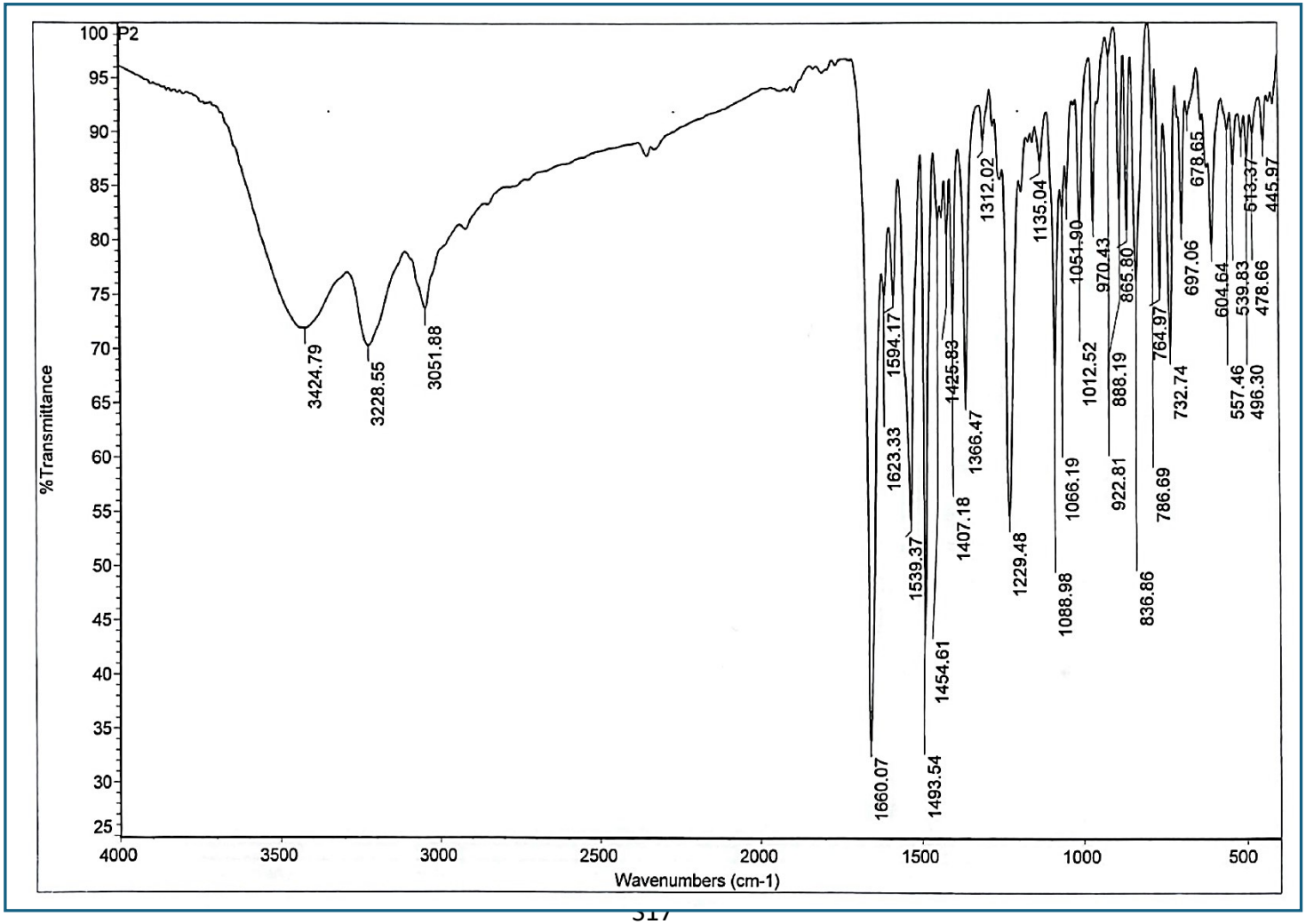
P2
%Transmittance
Wavenumbers (cm-1)
100
95
90
85
80
75
70
65
60
55
50
45
40
35
30
25
4000
3500
3000
2500
2000
1500
1000
500
3424.79
3228.55
3051.88
1660.07
1623.33
1594.17
1539.37
1493.54
1454.61
1425.83
1407.18
1366.47
1312.02
1229.48
1135.04
1088.98
1066.19
1051.90
1012.52
970.43
922.81
888.19
865.80
836.86
786.69
764.97
732.74
697.06
678.65
604.64
557.46
539.83
496.30
478.66
445.97

FTIR spectrum of compound **3b**

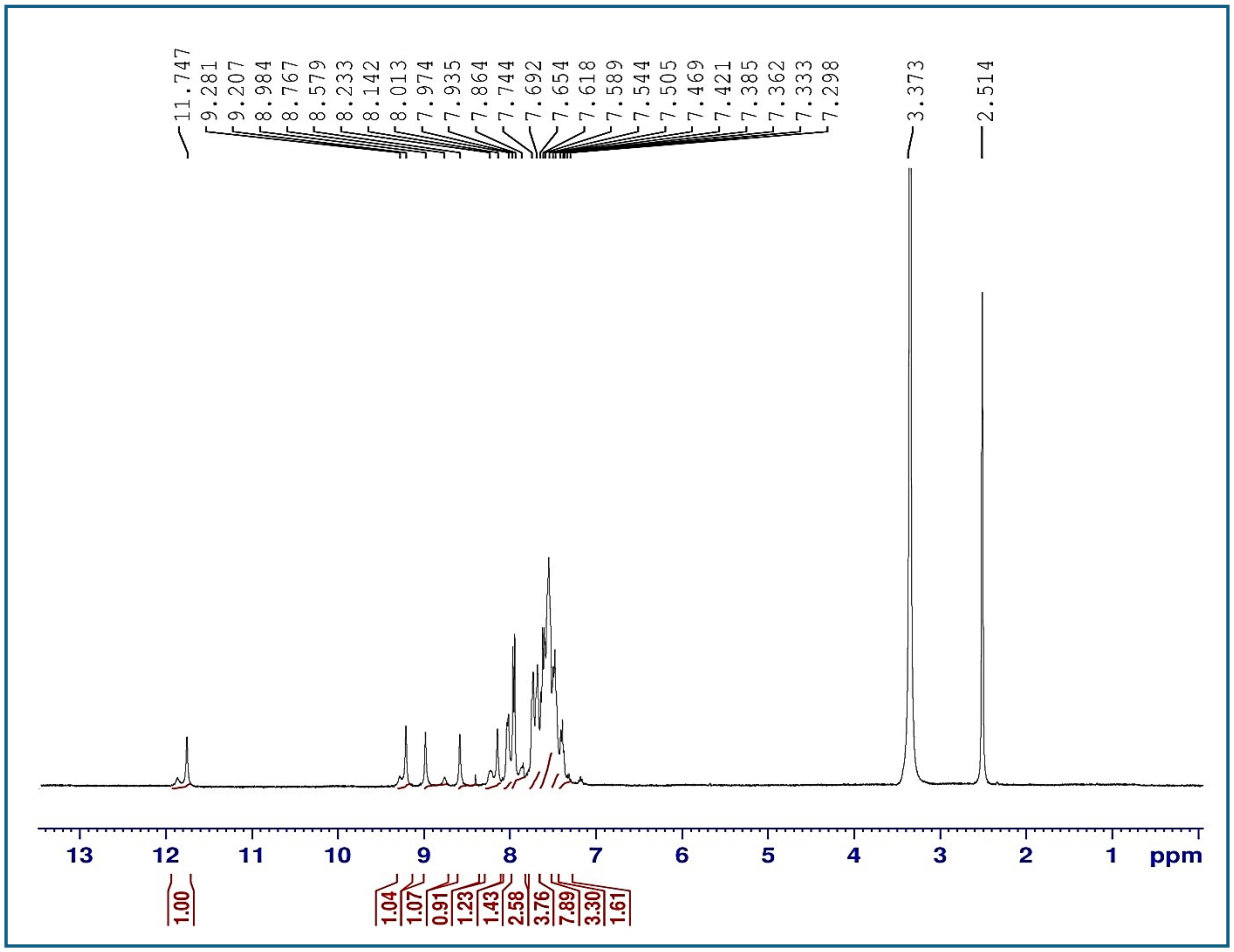

^{1}H NMR spectrum (DMSO-d_6) of compound **3b**

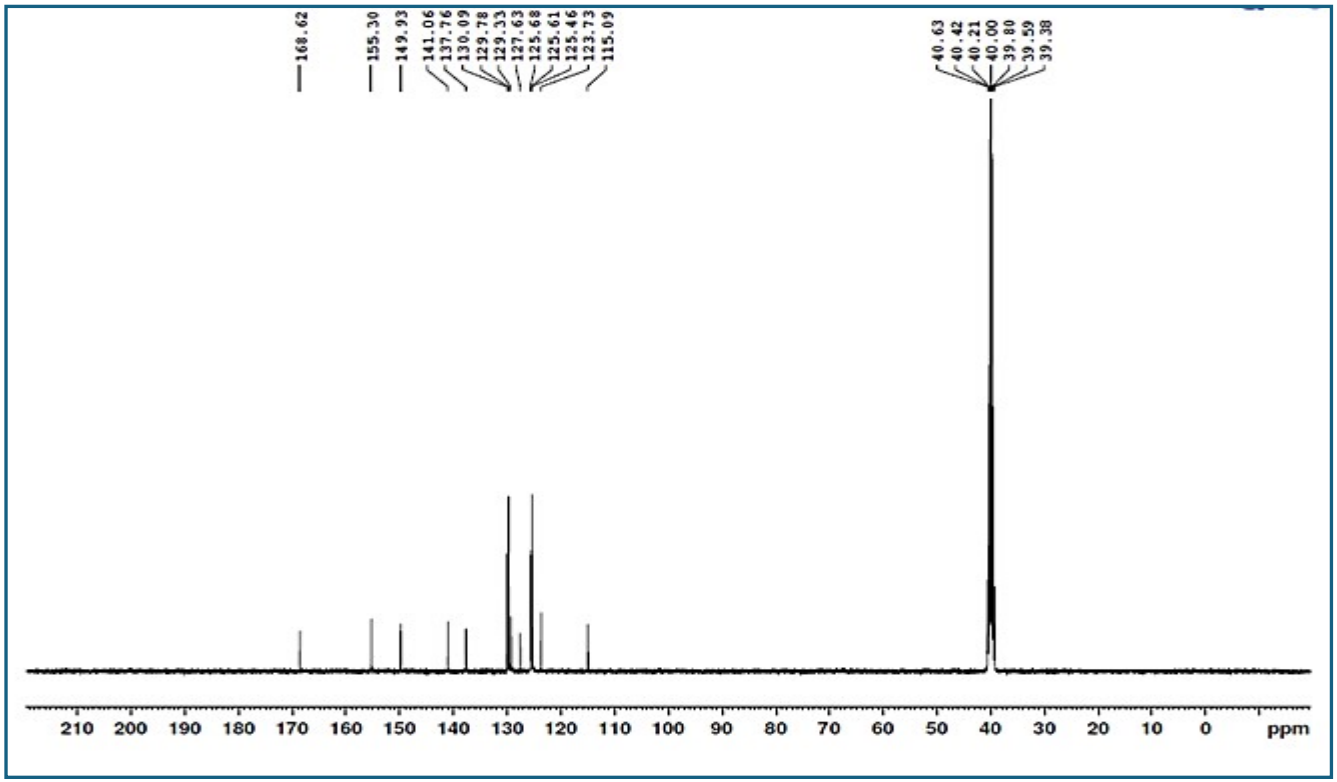

^{13}C NMR spectrum (DMSO-d_6) of compound **3b**

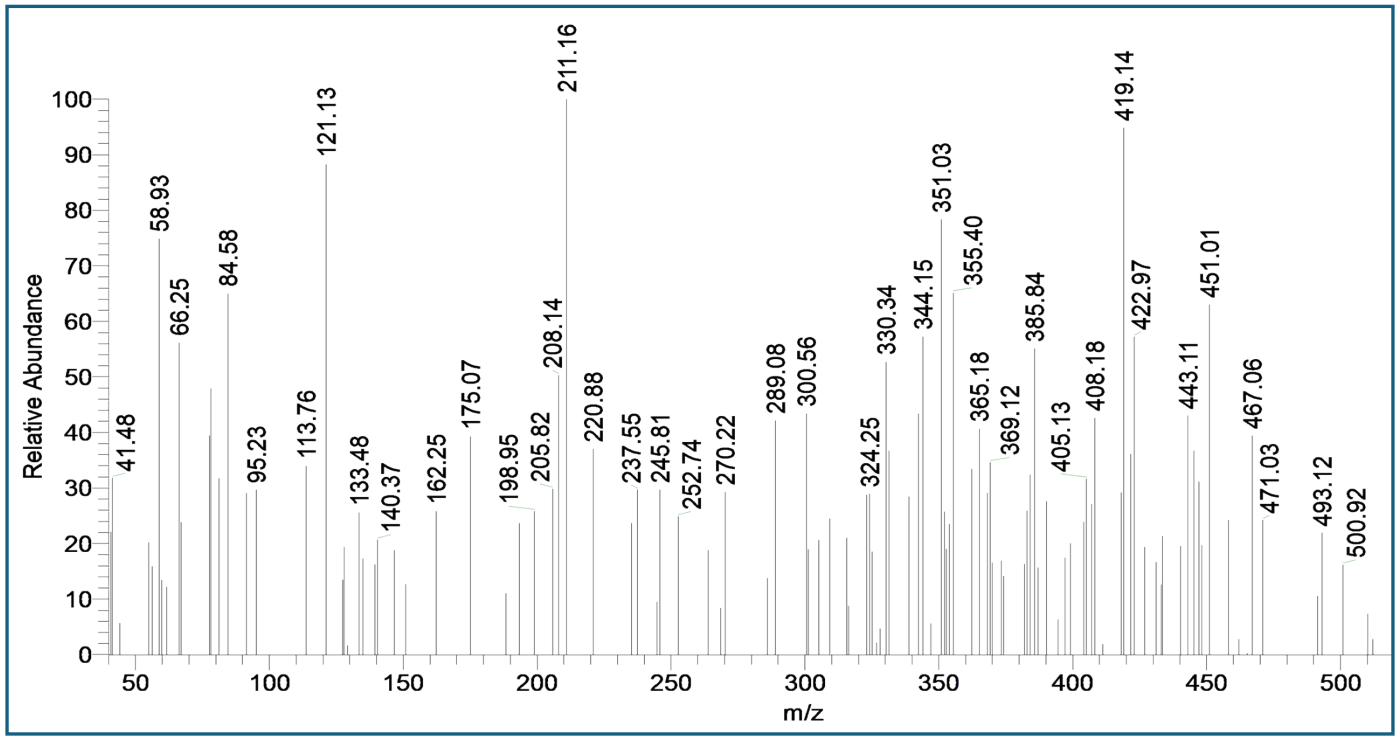

GCMS of compound **3b**

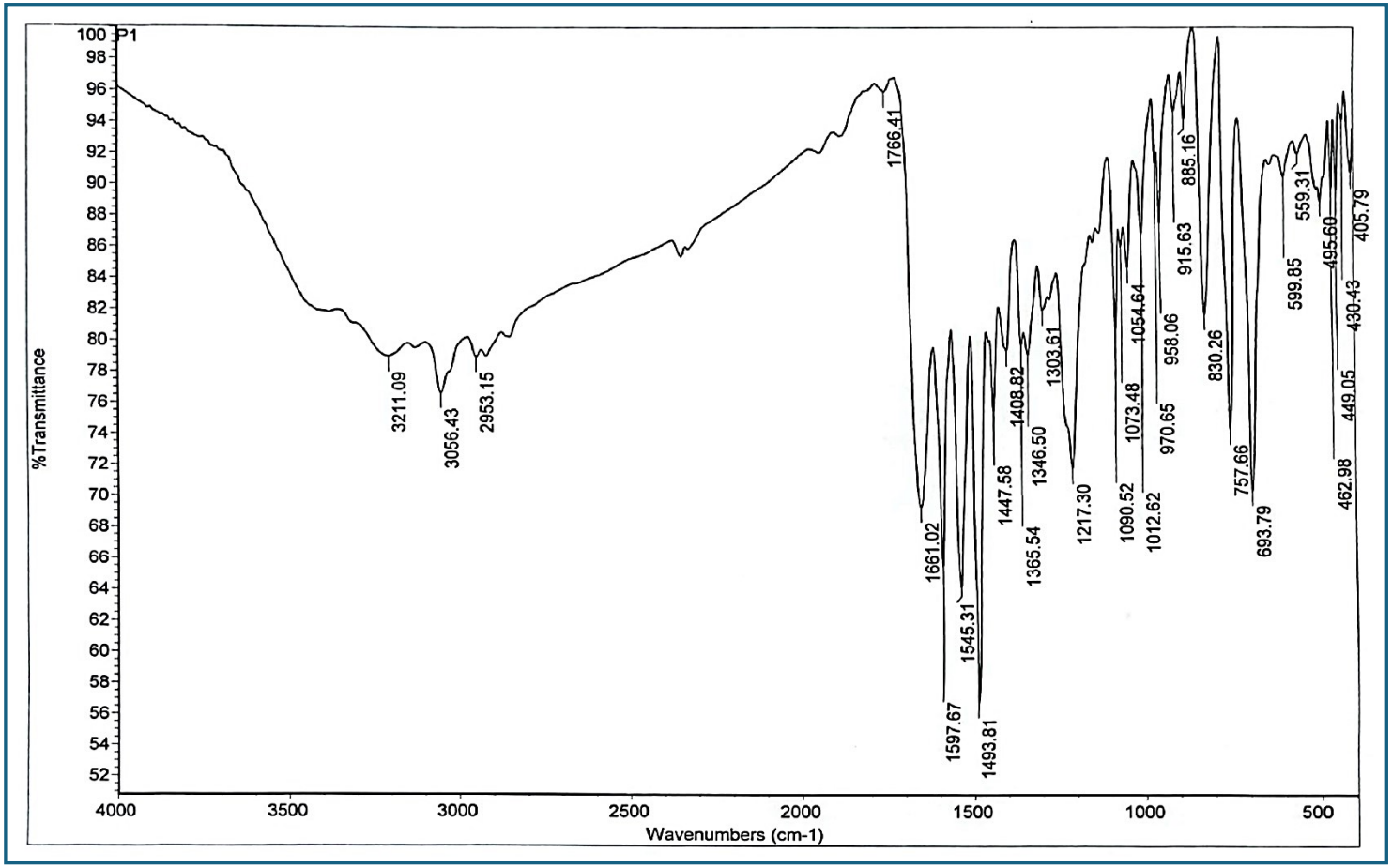
P1
%Transmittance
Wavenumbers (cm-1)
100
98
96
94
92
90
88
86
84
82
80
78
76
74
72
70
68
66
64
62
60
58
56
54
52
4000
3500
3000
2500
2000
1500
1000
500
3211.09
3056.43
2953.15
1766.41
1661.02
1597.67
1545.31
1493.81
1447.58
1408.82
1365.54
1346.50
1303.61
1217.30
1090.52
1073.48
1054.64
1012.62
970.65
958.06
915.63
885.16
830.26
757.66
693.79
599.85
559.31
495.60
462.98
449.05
430.43
405.79

FTIR spectrum of compound **3c**

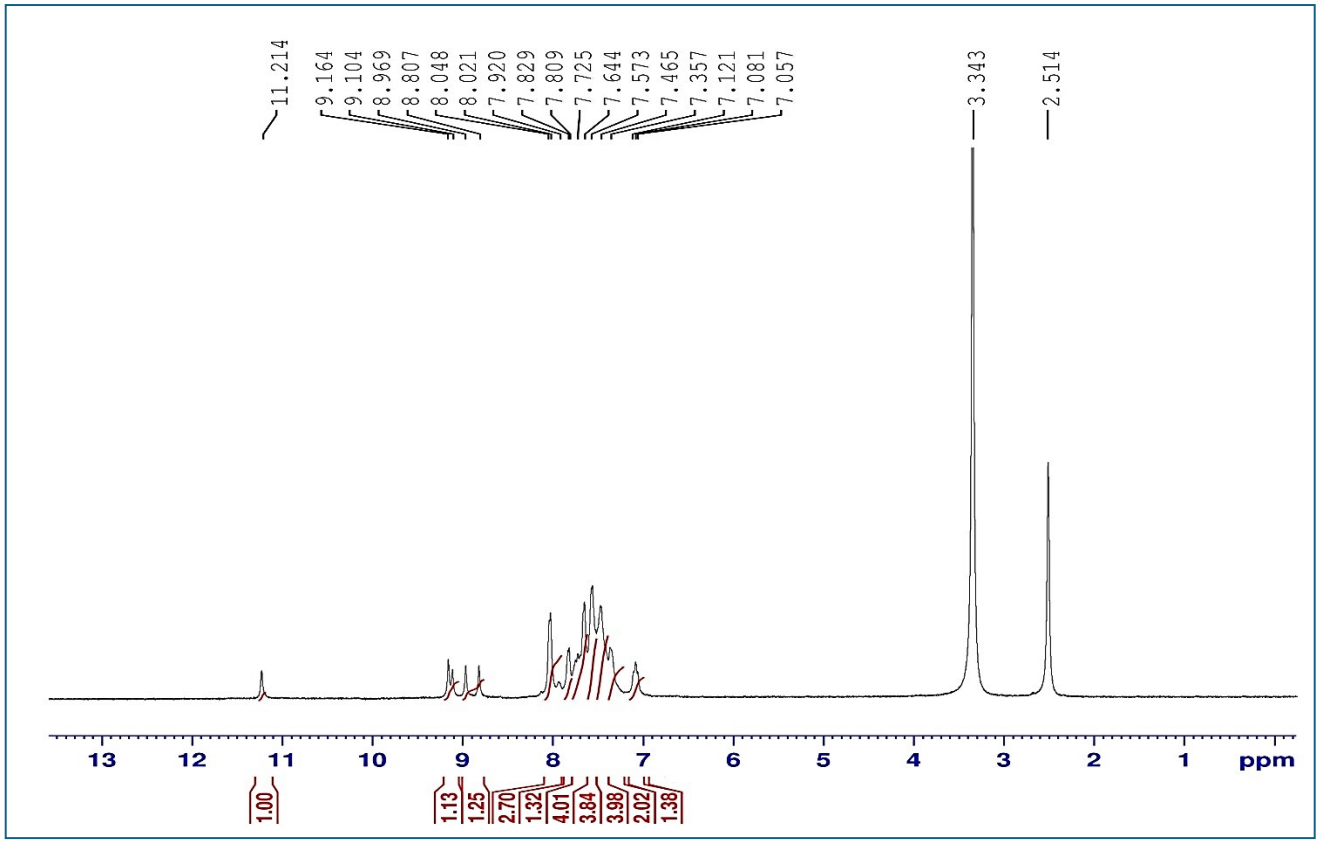

^{1}H NMR spectrum (DMSO-d_6) of compound **3c**

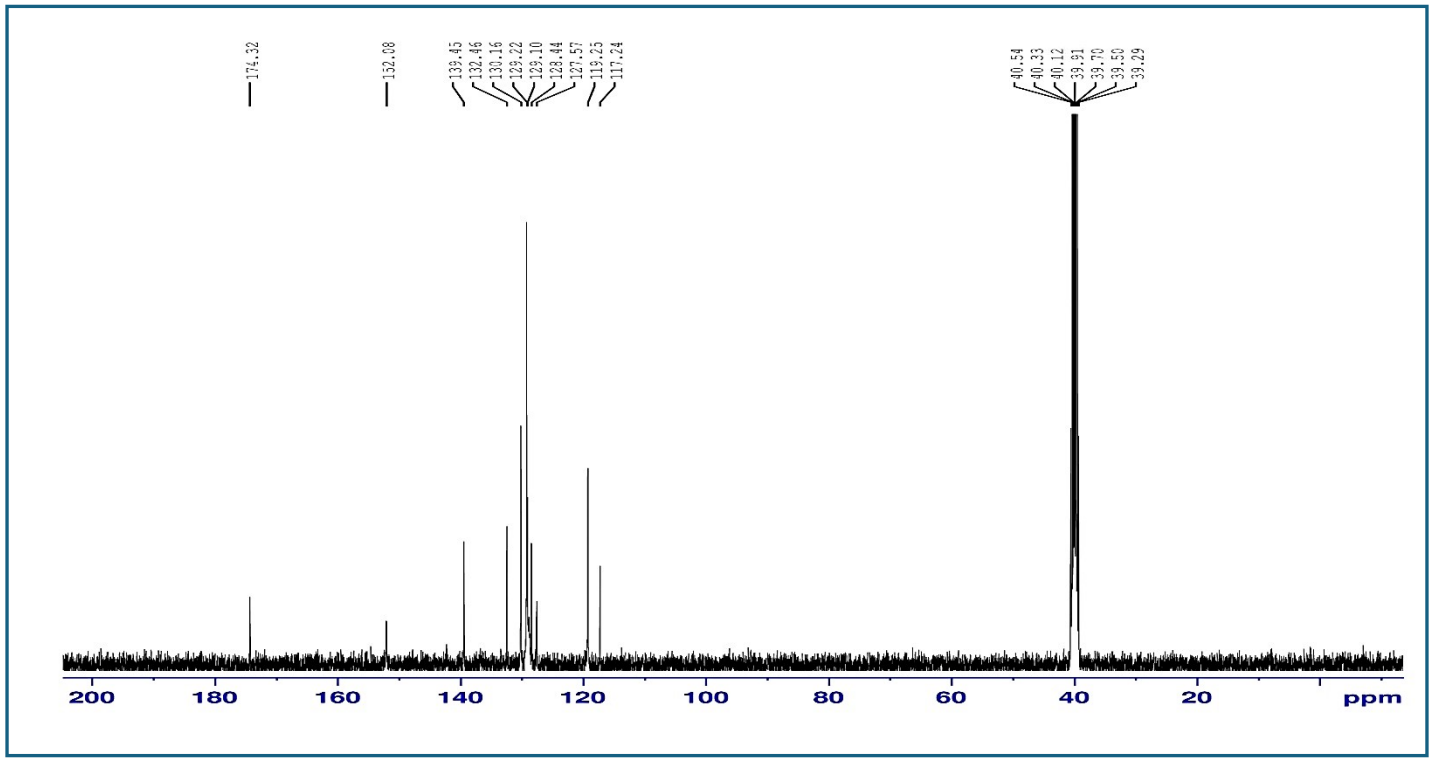

^{13}C NMR spectrum (DMSO-d_6) of compound **3c**

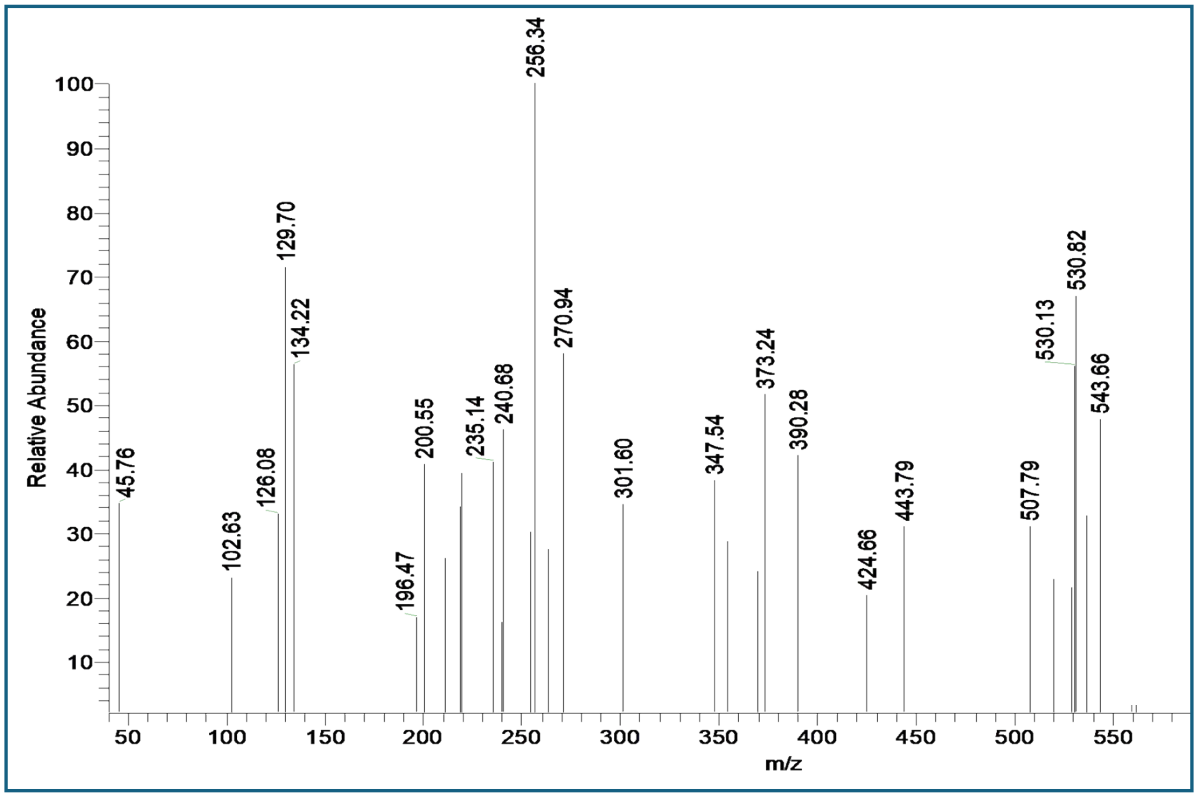

GCMS of compound **3c**